1942 *Inorg. Chem.* **2010**, *49*, 1942–1946
DOI: 10.1021/ic9023585

Inorganic Chemistry
Article

Hydrothermal Synthesis of Ytterbium Silicate Nanoparticles

Hongfei Chen,[†,‡] Yanfeng Gao,*[,†] Yun Liu,[†,‡] and Hongjie Luo[†]

[†] *Shanghai Institute of Ceramics (SIC), Chinese Academy of Sciences (CAS), 1295 Dingxi, Changning, Shanghai 200050, China, and* [‡] *Graduate University of Chinese Academy of Sciences, 19 Yuquanlu, Beijing, 100049, China*

Received November 28, 2009

A simple, low-cost hydrothermal method was developed to synthesize 20-nm-diameter single-crystalline ytterbium silicate ($Yb_2Si_2O_7$ and Yb_2SiO_5) nanoparticles at 200 °C. This is nearly 1000 °C lower than that for the typical sol−gel route to ytterbium silicate powders. Obtained powders showed very low thermal conductivity, a suitable thermal expansion coefficient, and excellent thermal/structural stability, suggesting a potential application to environmental and thermal barrier coatings. Special focus was placed on assessing the hydrothermal reaction mechanism for particle formation.

Intoduction

Silicon-based nonoxide structure ceramics, such as Si_3N_4 and SiC, have great potential for use as hot section components of gas turbine engines, owing to their superior high-temperature mechanical properties and durability. A major problem that limits the application of these materials is their environmental durability in high-velocity combustion environments that contain high-temperature water vapor.[1,2] An environmental barrier coating (EBC) must be deposited onto the composites to address this problem. Rare earth silicates, especially ytterbium silicate (i.e., Yb_2SiO_5 and $Yb_2Si_2O_7$), are excellent EBC materials, due to their superior high-temperature capability, outstanding durability in water vapor, and desirable chemical and mechanical compatibility with a silicon-based matrix.[3−5]

Solid-state reaction[6] and sol−gel syntheses[7−9] are two typical routes to the preparation of rare earth silicates, such as ytterbium silicate,[7] yttrium silicate,[9] and lutetium silicate.[6,8] However, it is difficult to obtain pure single-phase products, except at elevated synthesis temperatures or with complicated process parameters. Furthermore, products from the two methods usually consist of particles having large sizes and a wide size distribution.[7,9] This hinders the formation of a dense coating, making it easy for oxygen to diffuse through the EBC. Therefore, it is necessary to develop an easy, cost-effective, and efficient method to obtain fine powders with a narrow size distribution. The hydrothermal synthesis method is able to carefully control synthesis parameters and is a promising "soft-chemical" process for preparing low-dimensional nanostructured materials with high crystallinity as long as chemicals and modifiers are correctly selected.[10−12] A $NaReSi_xO_y$ compound is preferentially formed under hydrothermal conditions at a low temperature (< 200 °C) when NaOH is chosen as the precipitator,[13] due to the "bridge effect" of Na ions in the crystal growth. By using urea as a precipitator, only the amorphous Lu_2SiO_5 precursor was synthesized after hydrothermal treatment at 200 °C for 10 h because of the poor efficiency of urea to precipitate Si in the solution, and Lu_2SiO_5 was finally obtained by calcination at 1000 °C.[14] In the present work, in order to exploit a one-step hydrothermal route that can prepare ytterbium silicate nanoparticles, we systematically compared the aqua chemistry of Si and Yb and chose HCl and $NH_3 \cdot H_2O$ to precipitate Si and Yb, separately. Careful control of final pH values of the two precipitates and selecting a proper concentration of solution were also paid attention; neglecting either of them can lead to a failure result. In addition, the primary factors that affect the final products are discussed in detail. $Yb_2Si_2O_7$ and Yb_2SiO_5 nanoparticles, with a particle size range of 20−30 nm in diameter, have been successfully synthesized for the first time.

*To whom correspondence should be addressed. Tel./Fax: +86-21-5241-5270. E-mail: yfgao@mail.sic.ac.cn.

(1) Klemm, H. *J. Eur. Ceram. Soc.* **2002**, *22* (14−15), 2735−2740.
(2) Klemm, H.; Taut, C.; Wotting, G. *J. Eur. Ceram. Soc.* **2003**, *23* (4), 619−627.
(3) Lee, K. N.; Fox, D. S.; Bansal, N. P. *J. Eur. Ceram. Soc.* **2005**, *25* (10), 1705−1715.
(4) Ueno, S.; Ohji, T.; Lin, H. T. *Corros. Sci.* **2008**, *50* (1), 178−182.
(5) Maier, N.; Nickel, K. G.; Rixecker, G. *J. Eur. Ceram. Soc.* **2007**, *27* (7), 2705−2713.
(6) Ueno, S.; Lin, H. T.; Ohji, T. *J. Eur. Ceram. Soc.* **2008**, *28* (12), 2359−2361.
(7) Wen, H. M.; Dong, S. M.; He, P.; Wang, Z; Zhou, H. J.; Zhang, X. Y. *J. Am. Ceram. Soc.* **2007**, *90* (12), 4043−4046.
(8) Jayaseelan, D. D.; Ueno, S.; Ohji, T.; Kanzaki, S. *Mater. Chem. Phys.* **2004**, *84* (1), 192−195.
(9) Boyer, D.; Derby, B. *J. Am. Ceram. Soc.* **2003**, *86* (9), 1595−1597.
(10) Ge, S.; Shi, X.; Sun, K.; Li, C.; Uher, C.; Baker, J. R.; Banaszak Holl, M. M.; Orr, B. G. *J. Phys. Chem. C* **2009**, *113* (31), 13593−13599.
(11) Huang, Y.; You, H.; Jia, G.; Zheng, Y.; Song, Y.; Yang, M.; Liu, K.; Zhang, L. *J. Phys. Chem. C* **2009**, *113* (39), 16962−16968.
(12) Wang, W. W.; Yao, J. L. *J. Phys. Chem. C* **2009**, *113* (8), 3070−3075.
(13) Byrappa, K.; Yoshimura, M. *Handbook of Hydrothermal Technology: A Technology for Crystal Growth and Materials Processing*; Noyes Publications/William Andrew Publishing, LLC: Norwich, NY, 2001.
(14) Yun, P.; Shi, Y.; Zhou, D.; Xie, J. *J. Rare Earths* (*Engl. Ed.*) **2009**, *27* (5), 801−805.

 Published on Web 01/19/2010

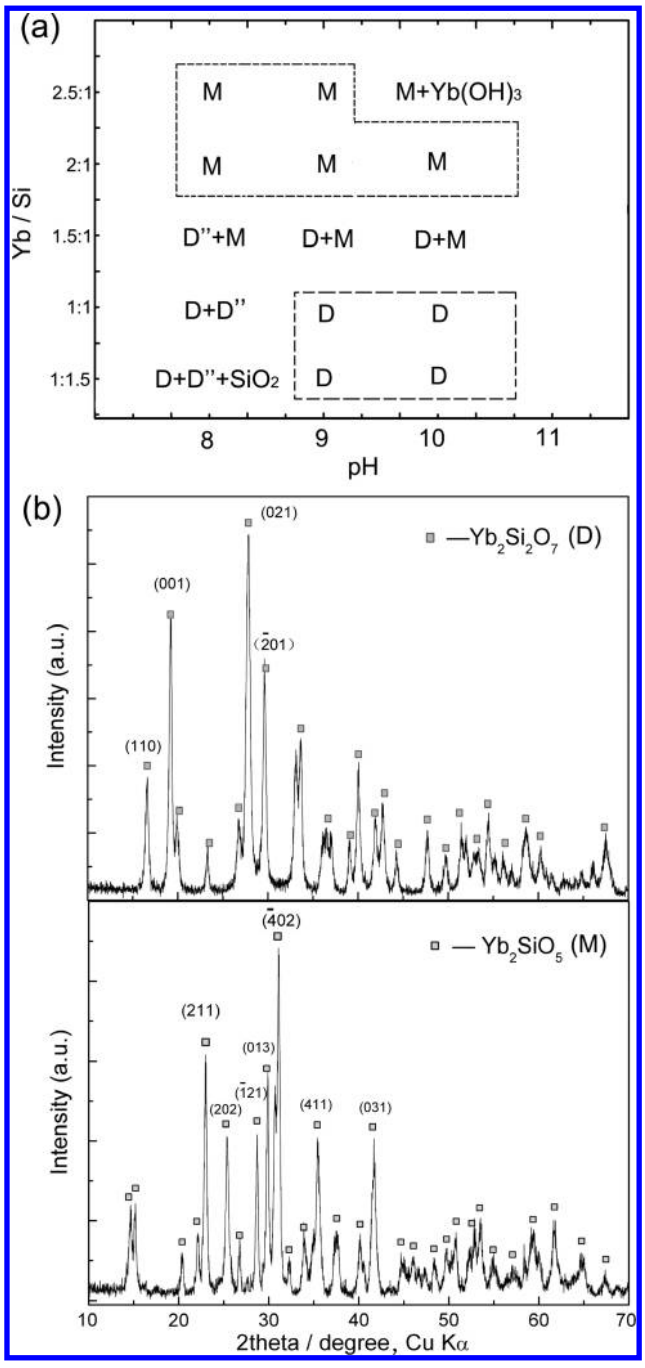

Figure 1. (a) The phase compositions obtained at different pH values and different molar ratios of starting materials. D refers to ytterbium disilicate with the space group $C2/m$, and D′′ refers to the intermediate phase of ytterbium disilicate with $C2$ symmetry (JCPDS No. 30-1438). M is ytterbium monosilicate, and SiO_2 (JCPDS No. 14-0654) came from an excess precipitate of Na_2SiO_3 at pH 8. (b) XRD patterns of $Yb_2Si_2O_7$ (D) and Yb_2SiO_5 (M) prepared at 200 °C, pH 9, with Yb/Si molar ratios of 1 and 2, respectively.

Two different phases, ytterbium disilicate (D) and ytterbium monosilicate (M), were synthesized by controlling the pH value and molar ratio of starting materials (Yb/Si, Figure 1a). As shown in the diagram, D and M phases were obtained over a wide range of pH values and Yb/Si ratios, other than a stoichiometric ratio. X-ray diffraction (XRD) patterns for the hydrothermal reaction products (200 °C, 6 h, pH 9) are shown in Figure 1b. The diffraction peaks can be assigned to Yb_2SiO_5 and $Yb_2Si_2O_7$ of the thortveitite structure, with a space group of $C2/m$ (JCPDS No. 25-1345). Figure 2 shows representative transmission electron microscopy (TEM) micrographs of the prepared $Yb_2Si_2O_7$ and Yb_2SiO_5 particles. The overview image of $Yb_2Si_2O_7$, shown in Figure 2a, illustrates that the sample entirely consisted of nanosized nearly monodispersed particles. Particles were quite uniform in size and shape. Typically, the mean diameter was about 20 nm. Crystallinity and phase were confirmed by electron diffraction analysis, which revealed diffraction spots for the thortveitite structure of a single crystalline $Yb_2Si_2O_7$ (Figure 2b). The high-resolution image of a single $Yb_2Si_2O_7$ nanoparticle, shown in Figure 2c, reveals sets of lattice fringes. This yields additional evidence that the particles were highly crystalline. Although the synthesis procedure was identical to that used for $Yb_2Si_2O_7$, the morphology of Yb_2SiO_5 particles was totally different, potentially indicating a different ion state in the solution during synthesis. These particles agglomerated into a polycrystalline flower-like structure with a mean diameter of about 30 nm for a single particle (Figure 2d).

Regarding the hydrothermal synthesis of ytterbium silicate (e.g., $Yb_2Si_2O_7$), it is believed that the temperature and the strong basic solution, from a high NH_4OH concentration, had a significant influence on the formation process. To a large extent, the temperature was a primary ingredient that determined the crystallinity, morphology, and size distribution of the nanoparticles. A kinetic model that is based on nucleation (dN/dt) and growth rate (dG/dt) can describe these factors.[13]

$$dN/dt = A(T)\{\exp[E(T)\cdot t]^{-1}\} \quad (1)$$

$$dG/dt = K(T)\,t \quad (2)$$

In these equations, all of the coefficients (A, E, and K) increased with the temperature, revealing that both the rate of nucleation (eq 1) and linear rate of crystal growth (eq 2) increase with increasing temperature. The competition of nucleation and growth affected the morphology and size distribution. The formation of fine nanoparticles suggests that quick self-nucleation can occur under all of the reaction conditions.[15] However, the subsequent growth step seemed very short at temperatures below 190 °C within a 6 h reaction. This is because some irregular particles, with a small size of 10 nm, were observed, as shown in Figure 3a. Consequently, the kinetic curve increased progressively and the growth area was very small (curve 2 in Figure 3b). When the synthesis temperature was elevated (e.g., 200 °C), the time for the nucleation step was greatly shortened, as according to eq 1. Thus, the reaction quickly moved to the growth step with a higher $K(T)$ value (eq 2) and a consequent bigger size of particles. From another point of view, the driving force of nucleation and growth at a high temperature correspondingly increased, which improved the activity of monomers in the solution. In a diffusion-controlled hydrothermal system,[16] the increase of the diffusion rate of monomers would facilitate a higher probability of collision of the monomers. Therefore, it made particles easier to grow larger than that at a low temperature.

(15) Bartell, L. S. *J. Phys. Chem. A* **2002**, *106* (45), 10893−10897.
(16) Huang, F.; Zhang, H. Z.; Banfield, J. F. *Nano Lett.* **2003**, *3* (3), 373−378.

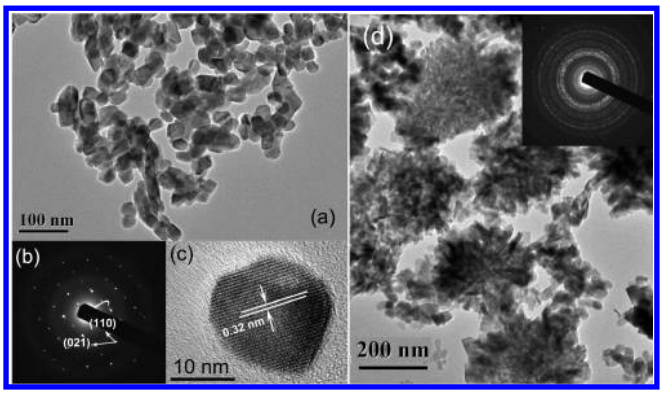

Figure 2. Representative TEM photographs of $Yb_2Si_2O_7$ and Yb_2SiO_5 particles obtained at 200 °C, pH 9, with Yb/Si molar ratios of 1 and 2, respectively: (a) an overview image, (b) selected area electronic diffraction (SAED) pattern of c, (c) high-resolution TEM image of a single $Yb_2Si_2O_7$ nanoparticle, (d) an overview image of Yb_2SiO_5 particles. The inset shows a SAED pattern of the Yb_2SiO_5 particles.

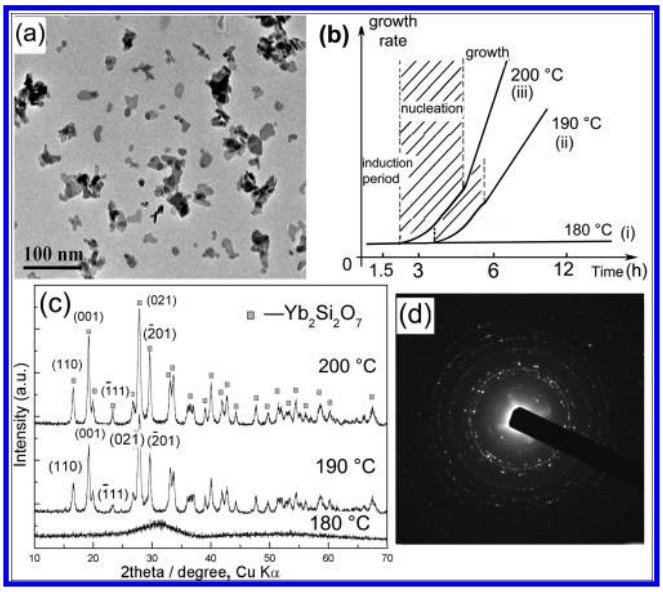

Figure 3. (a) TEM image of $Yb_2Si_2O_7$ nanoparticles prepared at 190 °C, pH 9, after reaction for 6 h, Yb/Si = 1 (molar ratio). (b) Kinetic curves of hydrothermal synthesis at different temperatures. (c) XRD patterns of as-synthesized $Yb_2Si_2O_7$ at pH 9 at different temperatures after reaction for 6 h, Yb/Si = 1. (d) SAED pattern of image a.

Increasing the temperature induced the amorphous−crystalline transformation. In our experiment, three different synthesis temperatures (i.e., 180, 190, and 200 °C) were employed (Figure 3c). At 180 °C, the as-obtained product was amorphous, while at 190 and 200 °C, both patterns were assigned to the $Yb_2Si_2O_7$ phase (JCPDS No. 25-1345). The SAED pattern for powders obtained at 190 °C (Figure 3d) suggests polycrystalline characteristics. When the synthesis temperature was raised to 200 °C, the products were developed to single crystals. These particles (about 20 nm in diameter) tended to slightly agglomerate (Figure 2a).

To achieve a better understanding of crystal growth kinetics, the phase evolutions at 190 and 200 °C after different reaction times were also investigated. At 190 °C, the diffraction peaks can be clearly identified after reaction for 6 h (Figure SI-1, Supporting Information). The reaction time shortened to 3 h in the case of 200 °C (Figure SI-2, Supporting Information). The crystallinity change was not notable beyond 6 h, indicating that the particles had reached a steady state and ceased growing.

Yb ions were precipitated by reacting with OH^- to form hydroxides (eq 3); the reaction proceeding is dependent on the solution pH. Solution pH is also a key parameter that affects the charge property and coordination of ions in solution. In our work, Yb_2SiO_5 and $Yb_2Si_2O_7$ could be produced with an excess of Yb and Si, respectively. At a molar ratio of Yb/Si = 2.5, the products were $Yb(OH)_3$ and Yb_2SiO_5 at pH 10 (Figure 1a). At high pHs (e.g., pH = 10), adequate OH^- could combine with Yb^{3+} ions to form $Yb(OH)_3$. However, at pH 8 and 9, the only product was Yb_2SiO_5. The absence of expected $Yb(OH)_3$ suggests that excess Yb did not precipitate, but formed dissoluble hydrolysate, $Yb(OH)_x(NO_3)_{3-x}$,[17] which was further brought away during centrifugation. An opposite situation occurred when a ratio of Yb/Si = 1:1.5 was used. In this case, the excess Si did not form a precipitate at high pH (above 9) because the precipitate of Si (H_2SiO_3) is metastable under strong alkaline conditions; it can dissolve as long-chain polymers or colloidal particles that have an overall composition ranging between $Si_2O_5^{2-}$ and SiO_3^{2-} or a more negatively charged pyrosilicate ($Si_2O_7^{6-}$) or orthosilicate (SiO_4^{4-}) group depending on the molar ratio of SiO_2/OH^-.[18] To form $Yb_2Si_2O_7$ and Yb_2SiO_5 in this particular system, the expected reactions are as follows:

$$Yb^{3+} + 3OH^- \rightarrow Yb(OH)_3\downarrow \quad (3)$$

$$SiO_3^{2-} + 2H^+ \rightarrow H_2SiO_3\downarrow \quad (4)$$

$$H_2SiO_3 + 2Yb(OH)_3 \rightarrow Yb_2SiO_5 + 4H_2O \quad (5)$$

$$2H_2SiO_3 + 2Yb(OH)_3 \rightarrow Yb_2Si_2O_7 + 5H_2O \quad (6)$$

$$2H_2SiO_3 + 2OH^- \rightarrow Si_2O_5^{2-} + 3H_2O \quad (7)$$

$$Si_2O_5^{2-} + 4OH^- \rightarrow Si_2O_7^{6-} + 2H_2O \quad (8)$$

H_2SiO_3 was the hydrolysate of Na_2SiO_3, after reaction with HCl (eq 4). A general reaction equation for the formation of Yb_2SiO_5 and $Yb_2Si_2O_7$ can be expressed as eqs 5 and 6, in which some of the Si−O−Si bonds are broken by Yb^{3+} ions, forming Si−O−Yb bonds.[7] Formation of Yb_2SiO_5 was a one-step reaction with little influence by the pH value, as no intermediate products were observed in the pH range between 8 and 10 (Figure 1a). On the other hand, the synthesis of $Yb_2Si_2O_7$ took two steps. At pH 8, the hydrothermal reaction could proceed through eq 7 first; then, a part of the product $Si_2O_5^{2-}$ continuously reacted with OH^- to form $Si_2O_7^{6-}$ (eq 8). Finally, the products were transformed to $Yb_2Si_2O_7$ with the space group $C2/m$, as well as an intermediate phase of $Yb_2Si_2O_7$ (D″ phase in Figure 1a) with $C2$ symmetry (JCPDS No. 30-1438) according to the XRD

(17) Rich, R. L. *Inorganic Reactions in Water*; Springer: Berlin, 2007.
(18) Ikornikova, N. Y. *Crystallization Processes under Hydrothermal Conditions*; Consultants Bureau: New York, 1973.

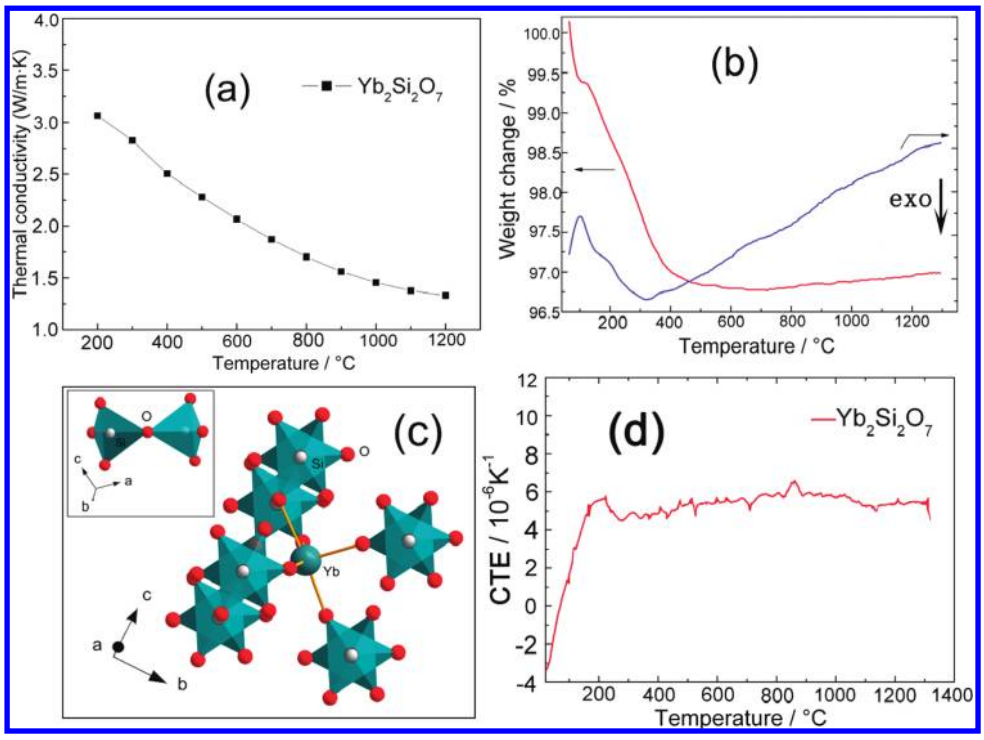

Figure 4. (a) Thermal conductivity of $Yb_2Si_2O_7$ powders prepared at 200 °C, pH 9, Yb/Si = 1 (molar ratio). (b) TG-DTA curves of $Yb_2Si_2O_7$ powders. (c) Crystal structure of thortveitite, $Yb_2Si_2O_7$; SiO_4 tetrahedron and Yb^{3+} cations bonded to the nonbridging oxygen atoms. Insert: Coordination of the Si and O. White spheres, Si; red spheres, O. (d) Thermal expansion coefficients of $Yb_2Si_2O_7$ powders prepared at 200 °C, pH 9, Yb/Si = 1.

pattern (Figure SI-3a, Supporting Information). The D″ phase seemed stable under the experimental conditions, and it did not change to the D phase even after prolonging the synthetic time to 48 h at 200 °C. However, it was still unclear whether the transformation is possible at an elevated temperature. The TEM image of these products is shown in Figure SI-3b (Supporting Information). Some rod-shaped nanocrystals were observed to agglomerate into sunflower-like particles along with some dispersed small crystals. At pH 9, most of the $Si_2O_5^{2-}$ product continued to react with OH^- and finally resulted in the formation of $Yb_2Si_2O_7$. As mentioned above, when the predominant species became more negatively charged, the dispersion of products obtained at pH 9 was better than that at pH 8.

To investigate the thermophysical properties of ytterbium silicate, we chose $Yb_2Si_2O_7$ as our research object because of its good dispersion and small particle size, which is more favorable to the EBC performance. Figure 4 shows the thermal properties of $Yb_2Si_2O_7$. Its thermal conductivity was about 1.75 W m^{-1} K^{-1} over an elevated temperature range (Figure 4a), which is lower than that prepared by a solid-state method (~2.25 W m^{-1} K^{-1}),[19] mainly because of increased phonon scattering for nanoscale particles. In the thermogravimetry and differential thermal analysis (TG-DTA) curve (Figure 4b), after desorbing water in the temperature range of 110−300 °C, there were almost no weight changes and obvious endothermic or exothermic peaks from 400 to 1300 °C. This demonstrates that $Yb_2Si_2O_7$ possesses excellent thermal and structural stability. These characteristics can be attributed to its crystal structure, in which oxygen atoms are nearly hexagonal closest packing, containing Yb cations in octahedral holes and silicon in tetrahedral holes over alternating parallel layers (001) (Figure 4c).[20,21] This wide range of stability makes it suitable for use in EBCs. The silicon-based nonoxide ceramics used in turbines have a CTE from 3.7 to 5.5 × 10^{-6} K^{-1} (3.7 × 10^{-6} K^{-1} for Si_3N_4, 4.7 × 10^{-6} K^{-1} for α-SiC, and 5.1 × 10^{-6} K^{-1} for β-SiC).[22] In Figure 4d, $Yb_2Si_2O_7$ has a CTE of ~4.5 × 10^{-6} K^{-1}. A very similar CTE is noticed between $Yb_2Si_2O_7$ and substrate ceramics, guaranteeing a low thermal stress at the coating and substrate interfaces and thereby a good thermal cycling resistance.

In summary, single-crystalline $Yb_2Si_2O_7$ nanoparticles and Yb_2SiO_5 were selectively synthesized using a hydrothermal method, and the formation mechanism was investigated. Two principal factors, the synthesis temperature and pH value, have great influence on the crystallinity, composition, and morphology of the products. $Yb_2Si_2O_7$ showed excellent heat insulation and desirable thermal and structural stability, signifying the potential for application in TBC/EBCs. Further studies of other rare-earth disilicates/monosilicates and control of their morphologies to achieve better properties are underway.

Synthesis

In a typical synthesis, ytterbium nitrate ($Yb(NO_3)_3 \cdot 6H_2O$) and sodium silicate ($Na_2SiO_3 \cdot 9H_2O$) were dissolved in 50 mL of distilled water to form 0.1 M solutions, separately. A total of ~8 mL of HCl (2 M) was added into the Na_2SiO_3 solution, and ~20 mL of diluted ammonia was dropped into the $Yb(NO_3)_3$ solution, both under strong stirring. After the reactions, two gel-like products with respective pH values of

(19) Ueno, S.; Jayaseelan, D. D.; Ohji, T. *Int. J. Appl. Ceram. Technol.* **2004**, *1* (4), 362−373.

(20) Bretheau-Raynal, F.; Lance, M.; Charpin, P. *J. Appl. Crys.* **1981**, *14*, 349−350.

(21) Felsche, J. *The Crystal Chemistry of the Rare-Earth Silicates*; Springer: Berlin, 1973.

(22) Sun, Z.; Li, M.; Zhou, Y. *J. Eur. Ceram. Soc.* **2009**, *29*, 551−557.

1.1 and 10.2 were mixed together. The final pH was adjusted to a certain value (8, 9, and 10) by adding extra ammonia. After aging for 3 h, the mixed solution was sealed in a 150 mL autoclave linear with a filling ratio of 70% and was slowly heated to a proper temperature (180, 190, 200 °C) for different time spans (1.5, 3, 6, 12 h).

Characterization

The phase compositions were identified by XRD (CuKα), using a D/max diffractometer (Rigaku, Japan), and the XRD patterns were analyzed using MDI Jade 5.0 software. The particle size and grain morphology of the powders were observed by TEM (Model JEM 2100F, JEOL, Tokyo, Japan) working at an accelerating voltage of 200 kV. TG-DTA measurements were conducted on the as-prepared $Yb_2Si_2O_7$ powders using a thermogravimetric analyzer (Model STA 449C, Netzsch, Selb, Germany). The powder samples were heated in an air atmosphere at a rate of 5 °C min^{-1} up to 1300 °C. The thermal conductivity k was determined from the thermal diffusivity α and the specific heat capacity C_p, using the equation

$$k = C_p \cdot \alpha \cdot \rho$$

where ρ is the measured density of the sample, obtained by the Archimedes method with an immersion medium of distilled water. For thermal diffusivity measurement, the specimen was prepared to be disk-shaped, about 11 mm in diameter and 0.8 mm in thickness. The thermal diffusivity of the samples as a function of the temperature (in the range between 200 and 1200 °C) was measured by the laser-flash method in an argon atmosphere. Both the front and back sides of the specimen were coated with a thin layer of graphite to prevent the laser beam from direct transmission through the specimen. Values for the specific heat capacity were obtained from an investigation of powder specimens using DSC, working continuously at a scanning rate of 20 K min^{-1} from room temperature to 1200 °C (Model 404, Netzsch, Bayern, Germany) in a N_2 atmosphere. The coefficient of thermal expansion was obtained by measuring the temperature-dependent change of specimen length using a high-temperature dilatometer (Model 402, Netzsch) from room temperature to 1200 °C in the air. The specimen was prepared to be a cuboid with a size of 25 × 4 × 4 mm. Before measuring, the specimen was pretreated at 1200 °C for 30 min to relieve the processing stress. Values were continuously recorded at a scanning rate of 5 °C min^{-1} during heating, and they were corrected by using a standard material, sapphire, as a reference.

Acknowledgment. The authors gratefully acknowledge the help from the Inorganic Materials Analysis and Testing Center of the Shanghai Institute of Ceramics, Chinese Academy of Sciences. H.C. also thanks Dr. T. Yang for his helpful discussion and the drawing of Figure 4c. This work is supported in part by the Century Program (One-Hundred-Talent Program) and YYYJ-0810 of the CAS and by NSFC (50972156).

Supporting Information Available: XRD patterns of $Yb_2Si_2O_7$ for different time spans at 190 °C, pH 9, Yb/Si = 1 (molar ratio): (a) 24 h, (b) 12 h, (c) 6 h, (d) 3 h. XRD patterns of $Yb_2Si_2O_7$ for different time spans at 200 °C, pH 9, Yb/Si = 1 (molar ratio): (a) 12 h, (b) 6 h, (c) 3 h, (d) 1.5 h. XRD pattern of $Yb_2Si_2O_7$ prepared at 200 °C, pH 8, Yb/Si = 1 (molar ratio). TEM morphology of $Yb_2Si_2O_7$ prepared at 200 °C, pH 8, Yb/Si = 1. This material is available free of charge via the Internet at http://pubs.acs.org.